A&A 485, 807–811 (2008)
DOI: 10.1051/0004-6361:200809752

Astronomy & Astrophysics

XMM-Newton observations of the Small Magellanic Cloud: RX J0105.9-7203, a 726 s Be/X-ray binary pulsar★

P. Eger and F. Haberl

Max-Planck-Institut für extraterrestrische Physik, Giessenbachstraße, 85748 Garching, Germany
e-mail: peger@mpe.mpg.de

Received 10 March 2008 / Accepted 15 April 2008

ABSTRACT

Aims. To investigate the Be/X-ray binary candidate RX J0105.9-7203 in the Small Magellanic Cloud (SMC), we analysed twenty-two archival XMM-Newton observations around the calibration target 1E 0102.2-7218.

Methods. We performed spectral and temporal analyses on the EPIC data of fifteen observations. We disregarded the data of one observation due to high background. The data of the remaining six observations were used to derive upper limits for the flux, because the source intensity was below the detection limit.

Results. We detected X-ray pulsations from RX J0105.9-7203 with long periods ranging from 723 ± 2 s to 731 ± 1 s in almost all observations where the source luminosity was above 8.0×10^{34} erg s^{-1}. The pulse profiles show more complex features in earlier observations whereas only a broad main pulse is seen at later times. The X-ray spectrum is well modelled by a power-law with photon index 0.71 ± 0.13 and a moderate absorption with $N_{\rm H} = (4.6 \pm 3.0) \times 10^{21}$ cm^{-2}. However, during one observation the source was extremely high absorbed: $N_{\rm H} = (2.6 \pm 1.7) \times 10^{23}$ cm^{-2}. The longterm X-ray lightcurve (covering 7.5 years) shows variations by at least a factor of 2. A long period of relative brightness (~1300 days) until Nov. 2003 was followed by an interval when RX J0105.9-7203 was very faint or not detected at all. Timing analysis of OGLE data of the optical counterpart revealed peaks in the FFT power-spectrum at 2.35 and 3.2 days.

Key words. galaxies: Magellanic Clouds – galaxies: stellar content – stars: emission-line, Be – stars: neutron – X-rays: binaries

1. Introduction

The supernova remnant (SNR) 1E 0102.2-7218 is located in the north eastern part of the SMC and has been observed with XMM-Newton twenty-two times since April 2000 for calibration purposes. There are five known Be/X-ray binary pulsars in this field with pulse periods of 3.34 s (Yokogawa et al. 2003), 304.5 s (Macomb et al. 2003), 345.2 s (Israel et al. 2000), 455 s (Sasaki et al. 2001) and 1323 s (Haberl & Pietsch 2005). In this region two more ROSAT sources (RX J0101.6-7204 and RX J0105.9-7203) have been proposed as high mass X-ray binary (HMXB) candidates (Haberl & Sasaki 2000), based on correlations with optical catalogues, but no pulsations have been reported so far. The latter of these two sources also lies within the error circle of the ASCA source AX J0105.8-7203 which Yokogawa et al. (2003) also listed as a Be/X-ray binary candidate. Sasaki et al. (2003) were able to identify an emission line star (Meyssonnier & Azzopardi 1993, hereafter MA93) as the optical counterpart using the more accurate XMM-Newton position obtained from the 3rd calibration observation. However, they did not perform a timing analysis due to the low countrate. Shtykovskiy & Gilfanov (2005) detected RX J0105.9-7203 with XMM-Newton in October 2003 and listed it as a "likely HMXB candidate" based on its X-ray brightness and the color index of the optical counterpart.

Here we report on results from spectral and timing analyses of all archival XMM-Newton EPIC data available at this time that add RX J0105.9-7203 to the numerous X-ray binary pulsars known in the SMC. Furthermore we discuss the long term luminosity and pulsation history.

★ Based on observations with XMM-Newton, an ESA Science Mission with instruments and contributions directly funded by ESA Member states and the USA (NASA).

2. Data analysis and results

The region around the SNR 1E 0102.2-7218 has been observed repeatedly (twenty-two times so far) with XMM-Newton (Jansen et al. 2001) since the launch of the mission for calibration of the EPIC-MOS (Turner et al. 2001) and EPIC-PN (Strüder et al. 2001) cameras (see Table 1). For the X-ray analysis we used the XMM-Newton Science Analysis System (SAS) version 7.1.0 supported by tools from the FTOOLS package together with XSPEC version 11.3.2p for spectral modelling.

The ROSAT source RX J0105.9-7203 is in the field of view (FOV) of all those observations. An EPIC mosaic image is presented by Haberl & Pietsch (2008a) in which the source is seen between the SNRs 1E 0102.2-7218 and B0104-72.3 as a faint blue point source. After astrometric bore-sight correction (see also Haberl & Pietsch 2008b), we determined the position of the source in fifteen observations using the SAS standard maximum likelihood technique for source detection. The position with the smallest error (0.6″) was obtained from the observation on April 20, 2003: RA = 01 05 55.31 and Dec = −72 03 50.2 (J2000.0). In six observations RX J0105.9-7203 was not detected. We applied a background screening for source detection, spectral and timing analyses. The resulting net exposures as well as the durations of the common good time intervals (GTI) of the PN and MOS cameras (used for timing analysis, see below) are also listed in Table 1.

Table 1. Details of the XMM-Newton EPIC observations.

Observation ID	Start time	End time	Exposures[(1)] noScr/Spec/Timing PN	MOS1	MOS2
0123110201	2000-04-16 19:06:50	2000-04-17 01:27:02	19298 / 16118 / –	18794 / 17543 / –	18794 / 17549 / –
0123110301	2000-04-17 03:41:01	2000-04-17 09:44:33	18298 / 10996 / –	17794 / 11425 / –	17794 / 11414 / –
0135720601	2001-04-14 20:35:50	2001-04-15 06:00:17	16198 / 9500 / 9500	32894 / 26134 / 9500	32894 / 26126 / 9500
0135720801	2001-12-25 17:58:49	2001-12-26 03:44:30	–	32127 / 29378 / 29377	32127 / 29394 / 29377
0135721001	2002-05-18 10:15:27	2002-05-18 19:45:51	12214 / 10871 / 10258	16684 / 10268 / 10258	14884 / 10257 / 10258
0135721101	2002-10-13 03:01:34	2002-10-13 09:58:53	–	23672 / 23269 / 23268	23672 / 23271 / 23268
0135721301	2002-12-14 03:35:52	2002-12-14 11:55:52	–	28672 / 28318 / 28274	28672 / 28310 / 28274
0135721401	2003-04-20 11:46:51	2003-04-21 00:42:41	–	34530 / 34498 / 34492	34529 / 34504 / 34492
0135721501	2003-10-27 07:37:01	2003-10-27 16:22:31	28534 / 26948 / 26094	30172 / 26965 / 26094	30177 / 26995 / 26094
0135721701	2003-11-16 05:54:00	2003-11-16 15:03:20	25975 / 25549 / 24834	27300 / 24859 / 24834	27300 / 24900 / 24834
0135721901	2004-04-28 06:51:55	2004-04-28 16:28:37	–	33274 / 31617 / –	33279 / 31639 / –
0135722401[(2)]	2004-10-14 08:45:59	2004-10-14 7:42:39	–	30872 / 30149 / –	30877 / 30063 / –
0135722001[(2)]	2004-10-26 06:38:37	2004-10-26 15:48:37	–	31672 / 29356 / –	–
0135722101[(2)]	2004-11-06 22:20:01	2004-11-06 12:28:21	29935 / 20288 / –	31572 / 22519 / –	31577 / 22503 / –
0135722201	not used due to high background				
0135722301[(2)]	2004-11-07 22:17:44	2004-11-08 07:27:07	29998 / 17895 / –	31635 / 21156 / –	31640 / 21172 / –
0135722501[(2)]	2005-04-17 21:57:56	2005-04-18 08:34:36	–	36872 / 21673 / –	36877 / 21664 / –
0135722601	2005-11-05 06:27:01	2005-11-05 15:12:30	–	–	30206 / 29538 / 29538
0135722701	2006-04-20 02:07:01	2006-04-20 10:52:31	–	30201 / 30201 / 30201	30206 / 30203 / 30201
0412980101	2006-11-05 00:37:16	2006-11-05 09:55:36	–	–	32177 / 31003 / 31003
0412980201[(2)]	2007-04-25 12:18:24	2007-04-25 22:43:24	–	36172 / 22514 / –	36177 / 22551 / –
0412980301	2007-10-26 09:31:06	2007-10-26 20:07:46	–	–	36877 / 33623 / –

[(1)] Exposure time without background screening/net exposure time with background screening (sum over all GTI) used for spectra, countrates or upper limits / net exposure time within the common PN/MOS GTI used for timing analysis (if performed). Only those instruments/modes where the source was within the FOV are listed. [(2)] Source within the FOV but not detected.

As reported by Sasaki et al. (2003), the emission line star [MA93] 1557 can be identified as the optical counterpart of RX J0105.9-7203 (Fig. 1). In Table 2 optical brightness and colours taken from the UBVR CCD Survey of the Magellanic Clouds (Massey 2002), the Magellanic Clouds Photometric Survey (MCPS, Zaritsky et al. 2002) and the OGLE *BVI* photometry catalogue (Udalski et al. 1998) are given.

To investigate long-term brightness variations of the optical counterpart we retrieved light curves in the *I*-band from the OGLE photometry database (star 137851; Szymanski 2005; Udalski et al. 1997). Unfortunately, there are no MACHO data available for this northern part of the SMC. The OGLE lightcurve (Fig. 2) shows a slight increase in luminosity over 3.5 years with additional variations by 0.1 mag superimposed.

We applied a Fast Fourier Transform (FFT) analysis to the OGLE *I*-band data (Lomb 1976; Scargle 1982) to determine whether these changes are periodic. Investigation of the period range between 2 days and 250 days (given by the longest uninterrupted data interval) revealed peaks at 2.35 and 3.2 days (see Fig. 3).

We searched for X-ray pulsations in the EPIC data for RX J0105.9-7203 in all observations that contain at least 200 source counts. After correcting the photon arrival times to the solar system barycenter, we combined the EPIC-PN and MOS data and accepted only those events within the common GTI of all three cameras (considering both instrument GTI and background screening). The source was not in the FOV of the PN camera when it was operated in large window (LW) or small window (SW) mode (see footnote to Table 1). FFT analyses revealed peaks around 726 s in the data from seven observations. The highest power was achieved in the energy band from 1 keV to 10 keV. To derive accurate values and errors for the period we used the Bayesian method (Gregory & Loredo 1996) as described in Zavlin et al. (2000). The results of our timing analysis can be found in Table 3 and Fig. 4 shows the power spectrum with the highest significance.

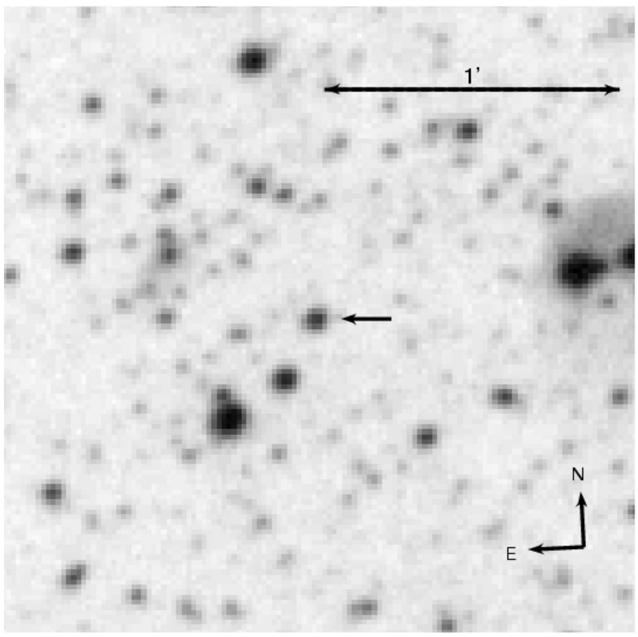

Fig. 1. Finding chart based on the DSS2 red image of the region around RX J0105.9-7203. The optical counterpart [MA93] 1557 is marked with an arrow. The positional error of the X-ray detection is smaller than the size of the star.

We folded the X-ray lightcurves on the best period in the standard EPIC energy bands (0.2−0.5 keV, 0.5−1.0 keV, 1.0−2.0 keV, 2.0−4.5 keV, 4.5−10.0 keV and the broad band

Table 2. Optical identification.

Source	Catalogue	RA and Dec (J2000.0)	*V* mag	*B* – *V*	*U* – *B*	*V* – *R*	*V* – *I*
RX J0105.9-7203	UBVR	01 05 55.19 –72 03 50.6	15.63	–0.02	–0.98	0.09	–
	MCPS	01 05 55.24 –72 03 50.3	15.70	–0.06	–1.14	–	0.13
	OGLE	01 05 55.23 –72 03 50.3	15.64	–0.05	–	–	0.18

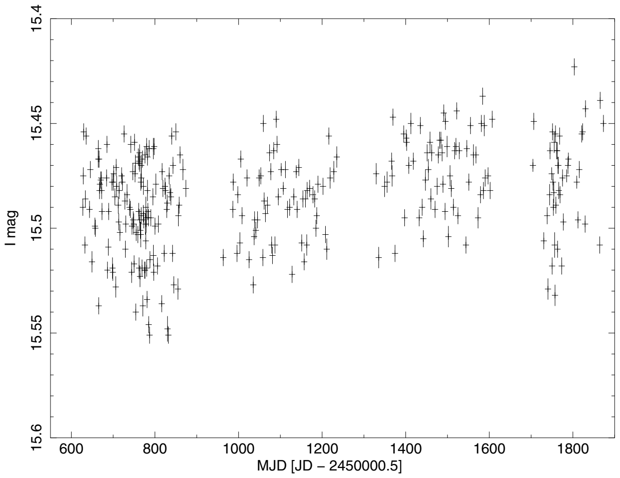

Fig. 2. OGLE *I*-band lightcurve for the optical counterpart of RX J0105.9-7203.

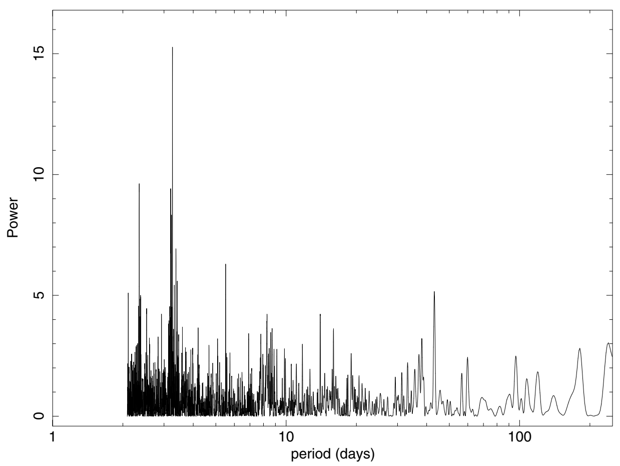

Fig. 3. Power spectrum of the optical counterpart of RX J0105.9-7203 produced from the OGLE *I*-band lightcurve.

0.2–10.0 keV) and plot two of the resulting pulse profiles from the observation where the source was brightest and that with the highest peak in the power-spectrum (Fig. 5). We show combined MOS data in the first panel, since PN data were only available for the latter observation.

For the analysis of the X-ray spectra we extracted pulse-phase averaged EPIC spectra for PN (single + double pixel events, PATTERN 0–4) and MOS (PATTERN 0–12) disregarding bad CCD pixels and columns (FLAG 0). Only those observations with at least 200 source counts (obs.: 3–10 and 18–20, see Table 1) were considered. At first only the EPIC spectra from the same observation were simultaneously fit with an absorbed power-law model only allowing for a normalization factor between the spectra. We used two absorption components, accounting for the Galactic foreground absorption (with a fixed hydrogen column density of 6×10^{20} cm^{-2} and elemental abundances from Wilms et al. 2000) and the SMC absorption (with

Table 3. Results from timing and spectral analysis of RX J0105.9-7203.

Date	FFT power	Pulsed fraction	Period[(2)] s	$L_X^{(3)}$ 10^{35} erg s^{-1}
2001-04-14[(1)]	11	(53 ± 41)%	722.8 ± 2.1	1.43 ± 0.27
2001-12-25	20	(62 ± 24)%	721.7 ± 1.2	0.76 ± 0.17
2002-10-13[(1)]	13	(47 ± 31)%	726.4 ± 5.0	1.58 ± 0.22
2002-12-14[(1)]	20	(44 ± 34)%	725.5 ± 3.3	1.46 ± 0.23
2003-04-20	40	(58 ± 26)%	728.7 ± 1.0	0.89 ± 0.23
2003-10-27	58	(59 ± 33)%	725.8 ± 1.2	0.88 ± 0.13
2003-11-16	26	(60 ± 20)%	731.2 ± 1.0	0.86 ± 0.17

[(1)] Period not significant and was found only after it was measured in other observations. [(2)] 1σ errors. [(3)] Intrinsic X-ray luminosity in the energy band 0.2–10.0 keV.

column density as a free parameter in the fit and with metal abundances reduced to 0.2 as typical for the SMC; Russell & Dopita 1992).

As a result we saw that both the SMC column density and photon index of all but the observation on April 20, 2006 (Fig. 6) were consistent within errors. In that one case the SMC absorption was exceptionally high: $N_H = (25.7 \pm 16.8) \times 10^{22}$ cm^{-2} and $\gamma = 1.22 \pm 0.65$. In a next step all consistent EPIC spectra (four PN, eight MOS1 and ten MOS2) were fit in parallel allowing again for a normalization factor. The best fit (reduced χ^2 = 1.44 for 134 degrees of freedom) yields an SMC absorption of $N_H = (4.6 \pm 3.0) \times 10^{21}$ cm^{-2} and a photon index of 0.71 ± 0.13. For clarity, we only show the best-fit on the brightest detection (Fig. 7). Using the ratio between flux and count-rate from the parallel fit we derived fluxes for those detections with less than 200 source counts by assuming the same spectral form. Upper limits for the flux in the six observations where RX J0105.9-7203 was not detected were calculated with the same method using sensitivity maps for count-rate estimates. With the known SMC distance (60 kpc) and the absorption set to zero, the fluxes translate into intrinsic source luminosities which are plotted in Fig. 8 and listed in Table 3 for the observations with period detection. We mainly show the MOS1 values (MOS2 when MOS1 data were not available, see Table 1 when this was the case), since RX J0105.9-7203 was not in the FOV of the PN camera in many observations. Errors for spectral parameters are at 90% condifdence levels.

3. Discussion

We report the discovery of pulsations with a long period of ~726 s from RX J0105.9-7203 in seven XMM-Newton observations and confirm a *V* ~ 15.6 mag star as the optical counterpart. The hard X-ray spectrum is well represented by a simple absorbed power-law, typical for Be/X-ray binary pulsars. Due to the relative faintness of the source (peak intrinsic luminostiy: 1.58×10^{35} erg s^{-1}) no more detailed spectral analysis is possible.

Following Coe et al. (2005), we estimate the spectral class of the optical counterpart from its *B* – *V* colour index to B0.5-B3,

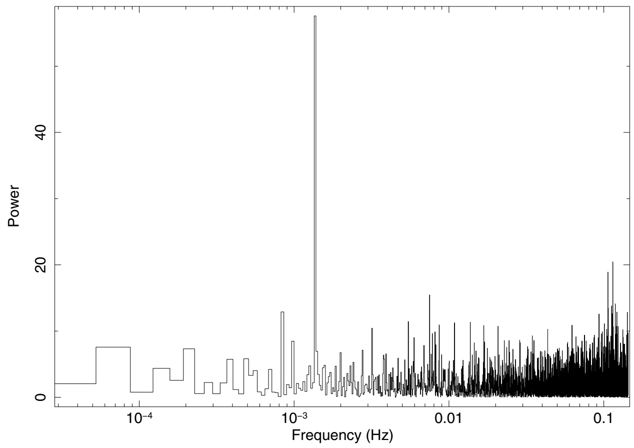

Fig. 4. Power spectrum of RX J0105.9-7203 produced from the 1.0−10.0 keV combined EPIC data of the observation on October 27, 2003.

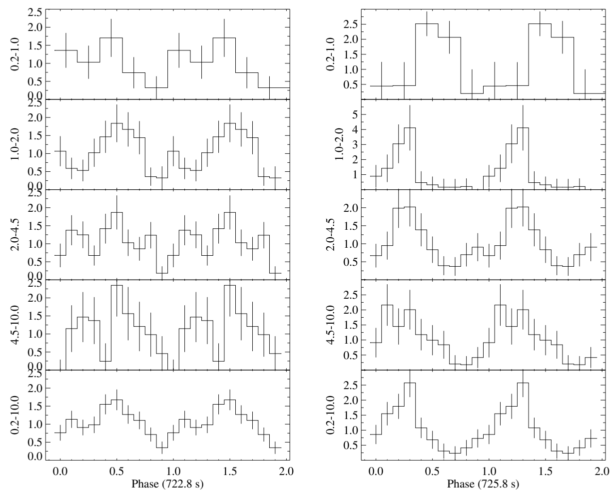

Fig. 5. Folded EPIC light curves of RX J0105.9-7203 taken from the observations on October 13, 2002 (*left*, MOS1+MOS2) and October 27, 2003 (*right*, PN) in the standard EPIC energy bands (the lower energy bands 0.2−0.5 keV and 0.5−1.0 keV were combined and re-binned by a factor of two due to low statistics. The panels show the pulse profiles for the different energies specified in keV. The intensity profiles are background subtracted and normalized to the average count rate (*left*: 0.013 cts/s and *right*: 0.006 cts/s) in the full bands.

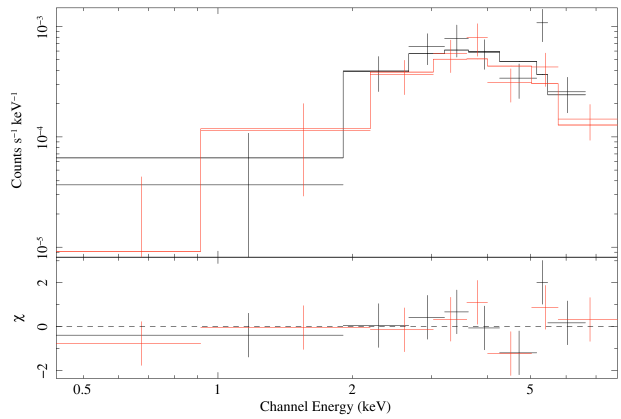

Fig. 6. The highly absorbed EPIC MOS1 (black) and MOS2 (red) spectra of RX J0105.9-7203 from the observation on April 20, 2006.

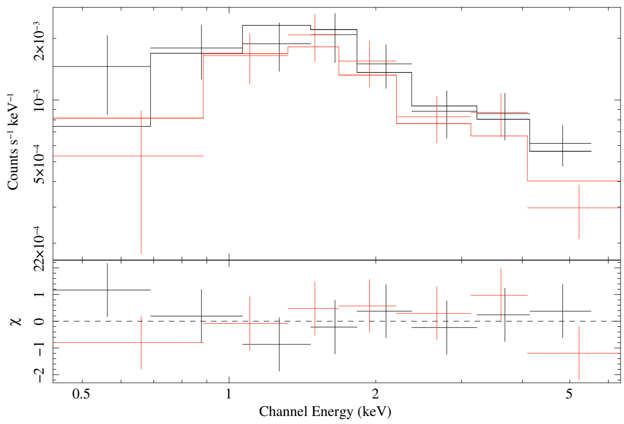

Fig. 7. EPIC MOS1 (black) and MOS2 (red) spectra of RX J0105.9-7203 from the observation on October 13, 2002, representative for all spectra used for parallel fitting.

depending on the observed $B-V$ index which is in the range −0.06 to −0.02 (Table 2). This assumes an extinction correction to the SMC of $E(B-V) = 0.08$ (Schwering & Israel 1991) and an additional correction of $(B-V) = -0.13$ to account for the presence of a circumstellar disc (Coe et al. 2005). The spectral types B0.5 to B2 are compatible with Be/X-ray binaries observed in the galaxy, whereas a spectral type of B3 (derived from the UBVR catalogue) may indicate that in this case the applied corrections for the circumstellar disc may have been insufficient. The difference between the $B-V$ values from the three photometric surveys suggests that the extinction varies with time. Changes in the matter distribution local to the binary system may account for these variations and are most likely due to changes in the disc of the Be star.

In the first half of the observations the long term X-ray lightcurve (Fig. 8) shows a long period of relative brightness (∼1300 days) followed by an interval when the source was either not detected (six observations) or was rather faint (four observations). However there is one exception in the second half (obs. from April 20, 2006, see note in Fig. 8) where RX J0105.9-7203 was relatively bright (1.30×10^{35} erg s^{-1}) but highly absorbed with $N_H = (25.7 \pm 16.8) \times 10^{22}$ cm^{-2}. This spectrum is seen in Fig. 6, and for comparison we show in Fig. 7 a typical moderately absorbed powerlaw, $N_H = (4.6 \pm 3.0) \times 10^{21}$ cm^{-2}, which we can fit to all other detetions. Similar variations in the N_H column density have also been reported from RX J0103.6-7201 (Haberl & Pietsch 2005) which is another long period pulsar in the same region. But, in contrast, we do not see a soft thermal component in the spectrum of RX J0105.9-7203.

The FFT power spectra of the X-ray data show no very significant peaks in the two observations where the source was brightest (October 13, 2002 and December 14, 2002), whereas the detection of pulsations becomes more significant in later observations until the maximum FFT power of 58 is reached, when the luminosity dropped to nearly half of its former value (see Table 3). This effect is not related to different exposure times (see Table 1). For a more detailed investigation we plotted the folded lightcurves of the two extreme cases in Fig. 5, where the left panel shows the observation (October 13, 2002) with the highest source luminosity, but rather low FFT power and the right panel the observation (October 27, 2003) with the highest power in the FFT spectrum. By fitting a sine plus its first harmonic to the profiles we derived pulsed fractions for the full energy band for each detecion (see Table 3) which are all consistent within their large errors. Due to the low statistics, we are not able to show

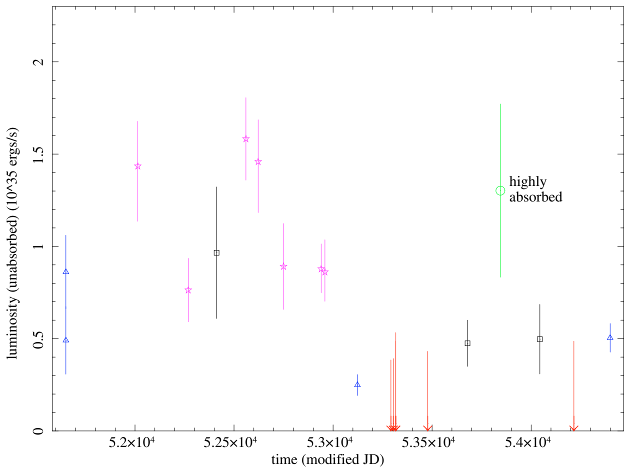

Fig. 8. Longterm X-ray lightcurve showing intrinsic source luminosities in the energy band 0.2−10.0 keV. Squares (black): used for parallel fitting, no pulsations found. Stars (magenta): used for parallel fitting, pulsations found. Triangles (blue): luminosity derived from countrate. Arrows (red): upper limits, source not detected. Circle (green): not used in parallel fitting, highly absorbed.

pulsed fractions for each of the different energy bands seperately. Additionally we see changes in the complexity of the pulse shape over time. A small peak between the main pulses appears during the earlier observation (left) whereas a much smoother profile is seen in the later detection (right). Furthermore there may be indications for a spin down of 3.2 s/year, since the period increased from 722.8 s to 731.2 s. However this is not very significant because all detected periods are consistent within 3σ errors.

From the relation between spin and orbital period (for a recent version of the "Corbet" diagram of SMC pulsars see Schmidtke & Cowley 2005), we expect an orbital period between ~63 days and ~251 days for RX J0105.9-7203. Short periods of a few days, as we detected in the I-band OGLE data of RX J0105.9-7203, are also seen in other SMC Be/X-ray binaries (Schmidtke et al. 2004; Schmidtke & Cowley 2005) and might be caused by a changing view of the Be disk region that is brightened by the neutron star or by non radial pulsations of the Be star.

Acknowledgements. The XMM-Newton project is supported by the Bundesministerium für Wirtschaft und Technologie/Deutsches Zentrum für Luft- und Raumfahrt (BMWI/DLR, FKZ 50 OX 0001) and the Max-Planck Society. The "Second Epoch Survey" of the southern sky was produced by the Anglo-Australian Observatory (AAO) using the UK Schmidt Telescope. Plates from this survey have been digitized and compressed by the ST ScI. Produced under Contract No. NAS 5-26555 with the National Aeronautics and Space Administration.

References

Coe, M. J., Edge, W. R. T., Galache, J. L., & McBride, V. A. 2005, MNRAS, 356, 502
Gregory, P. C., & Loredo, T. J. 1996, ApJ, 473, 1059
Haberl, F., & Sasaki, M. 2000, A&A, 359, 573
Haberl, F., & Pietsch, W. 2005, A&A, 438, 211
Haberl, F., & Pietsch, W. 2008a, in X-rays from Nearby Galaxies, MPE Rep., 295, 32 [arXiv:0712.2720]
Haberl, F., & Pietsch, W. 2008b, A&A, submitted
Israel, G. L., Campana, S., Covino, S., et al. 2000, ApJ, 531, L131
Jansen, F., Lumb, D., Altieri, B., et al. 2001, A&A, 365, L1
Lomb, N. R. 1976, Ap&SS, 39, 447
Macomb, D. J., Fox, D. W., Lamb, R. C., & Prince, T. A. 2003, ApJ, 584, L79
Massey, P. 2002, ApJS, 141, 81
Meyssonnier, N., & Azzopardi, M. 1993, A&AS, 102, 451
Russell, S. C., & Dopita, M. A. 1992, ApJ, 384, 508
Sasaki, M., Haberl, F., Keller, S., & Pietsch, W. 2001, A&A, 369, L29
Sasaki, M., Pietsch, W., & Haberl, F. 2003, A&A, 403, 901
Scargle, J. D. 1982, ApJ, 263, 835
Schmidtke, P. C., & Cowley, A. P. 2005, AJ, 130, 2220
Schmidtke, P. C., Cowley, A. P., Levenson, L., & Sweet, K. 2004, AJ, 127, 3388
Schwering, P. B. W., & Israel, F. P. 1991, A&A, 246, 231
Shtykovskiy, P., & Gilfanov, M. 2005, MNRAS, 362, 879
Strüder, L., Briel, U., Dennerl, K., et al. 2001, A&A, 365, L18
Szymanski, M. K. 2005, Acta Astron., 55, 43
Turner, M. J. L., Abbey, A., Arnaud, M., et al. 2001, A&A, 365, L27
Udalski, A., Kubiak, M., & Szymanski, M. 1997, Acta Astron., 47, 319
Udalski, A., Szymanski, M., Kubiak, M., et al. 1998, Acta Astron., 48, 147
Wilms, J., Allen, A., & McCray, R. 2000, ApJ, 542, 914
Yokogawa, J., Imanishi, K., Tsujimoto, M., Koyama, K., & Nishiuchi, M. 2003, PASJ, 55, 161
Zaritsky, D., Harris, J., Thompson, I. B., Grebel, E. K., & Massey, P. 2002, AJ, 123, 855
Zavlin, V. E., Pavlov, G. G., Sanwal, D., & Trümper, J. 2000, ApJ, 540, L25